THE JOURNAL OF PHYSICAL CHEMISTRY A
A JOURNAL OF THE AMERICAN CHEMICAL SOCIETY

pubs.acs.org/JPCA Article

Theoretical Study of the Reaction of the Methylidyne Radical (CH; $X^2\Pi$) with 1-Butyne (CH_3CH_2CCH; X^1A')

Anatoliy A. Nikolayev, Valeriy N. Azyazov, Ralf I. Kaiser, and Alexander M. Mebel*

Cite This: *J. Phys. Chem. A* 2021, 125, 9536–9547 Read Online

ACCESS | Metrics & More | Article Recommendations | Supporting Information

ABSTRACT: Ab initio CCSD(T)-F12/*cc*-pVTZ-f12//ωB97X-D/6-311G(d,p) + ZPE[ωB97X-D/6-311G(d,p)] calculations were carried out to unravel the area of the C_5H_7 potential energy surface accessed by the reaction of the methylidyne radical with 1-butyne. The results were utilized in Rice–Ramsperger–Kassel–Marcus calculations of the product branching ratios at the zero pressure limit. The preferable reaction mechanism has been shown to involve (nearly) instantaneous decomposition of the initial reaction adducts, whose structures are controlled by the isomeric form of the C_4H_6 reactant. If CH adds to the triple C≡C bond in the entrance reaction channel, the reaction is predicted to predominantly form the methylenecyclopropene + methyl (CH_3) and cyclopropenylidene + ethyl (C_2H_5) products roughly in a 2:1 ratio. CH insertion into a C–H bond in the methyl group of 1-butyne is anticipated to preferentially form ethylene + propargyl (C_3H_3) by the C–C bond β-scission in the initial complex, whereas CH insertion into C–H of the CH_2 group would predominantly produce vinylacetylene + methyl (CH_3) also by the C–C bond β-scission in the adduct. The barrierless and highly exoergic CH + 1-butyne reaction, facile in cold molecular clouds, is not likely to lead to the carbon skeleton molecular growth but generates C_4H_4 isomers methylenecyclopropene, vinylacetylene, and 1,2,3-butatriene and smaller C_2 and C_3 hydrocarbons such as methyl, ethyl, and propargyl radicals, ethylene, and cyclopropenylidene.

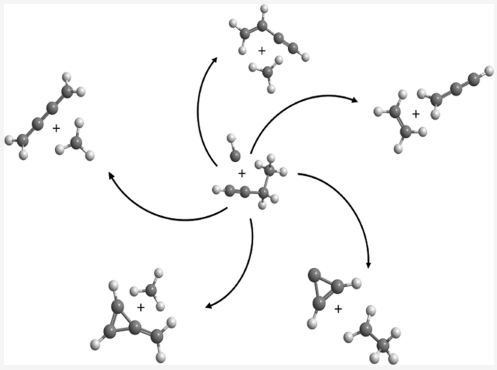

■ INTRODUCTION

Unsaturated C_5 hydrocarbons are of great interest for the physical, theoretical, and combustion chemistry and astrochemistry because they can serve as potential precursors to polycyclic aromatic hydrocarbons (PAHs) both in high-temperature environments, such as in combustion flames and circumstellar envelopes of dying carbon stars (IRC +10216), and under ultracold conditions, for example, in cold molecular clouds like TMC-1 and OMC-1.[1−22] For instance, high concentrations of C_5 species have been observed in fuel-rich flames.[1−3] The most systematic study of hydrocarbon-rich flames with allene and propyne, cyclopentene, and benzene as the fuels by Hansen and co-workers has identified, by means of molecular-beam mass spectrometry sampling *via* tunable vacuum ultraviolet (VUV) synchrotron photoionization, the presence of a broad range of C_5H_x molecules (x = 2–6, and 8), including C_5H_2 (1,2-cyclopentadien-4-yne), C_5H_3 (2,4-pentadiynyl-1, 1,4-pentadiynyl-3, and cyclopenta-1,2,3-triene radicals), C_5H_4 (1,2,3,4-pentatetraene, penta-1,2-dien-4-yne, 1,3-pentadiyne, and 1,4-pentadiyne), C_5H_5 (cyclopentadienyl radical), C_5H_6 (1,3-cyclopentadiene, 1-penten-3-yne, 3-penten-1-yne, and pent-1-en-4-yne), and C_5H_8 (1,3-pentadiene, cyclopentene, 2-pentyne, and 1,4-pentadiene).[1,2] Two C_5H_3 isomers (2,4-pentadiynyl-1 and 1,4-pentadiynyl-3) and two C_5H_5 isomers (1-vinylpropargyl and cyclopentadienyl, *c*-C_5H_5) were also detected in benzene/oxygen flames.[3] Alternatively, in deep space, the highly reactive pentynylidyne radical (C_5H) and the C_5 molecule have been discovered in the envelope of the carbon star IRC+10216;[4−7] the former has also been synthesized in the laboratory *via* crossed molecular beams of ground-state carbon atoms [$C(^3P)$] and diacetylene (C_4H_2).[23] Previously, experimental and theoretical studies of this and other groups have demonstrated that the C_5H_x species (x = 3–6) can be produced via neutral–neutral bimolecular reactions, such as $C(^3P)$ + C_4H_4 (vinylacetylene) → C_5H_3 + H, $C_2(X^1\Sigma_g/a^3\Pi_u)$ + C_3H_4 (methylacetylene and allene) → C_5H_3 + H, $C_2(X^1\Sigma_g/a^3\Pi_u)$ + C_4H_6 (1-butyne) → C_5H_3 + CH_3, C_3H_3 (1-propynyl) + C_2H_2 (acetylene) → C_5H_4 + H, C_3H_3 (propargyl) + C_2H_2 (acetylene) → C_5H_5 (cyclopentadienyl and 1-vinylpropargyl), $C(^3P)$ + C_4H_6 (1,3-butadiene, 1,2-butadiene, and dimethylacetylene) → C_5H_5 + H, $C_2(X^1\Sigma_g/a^3\Pi_u)$ + C_3H_6 (propylene) → C_5H_5 + H, C_2H (ethynyl) + C_3H_6 (propylene) → C_5H_6 + H.[8−21] The potential energy surfaces (PES) explored in these studies are very complex,

Received: August 24, 2021
Revised: September 25, 2021
Published: October 21, 2021

https://doi.org/10.1021/acs.jpca.1c07519
J. Phys. Chem. A 2021, 125, 9536–9547

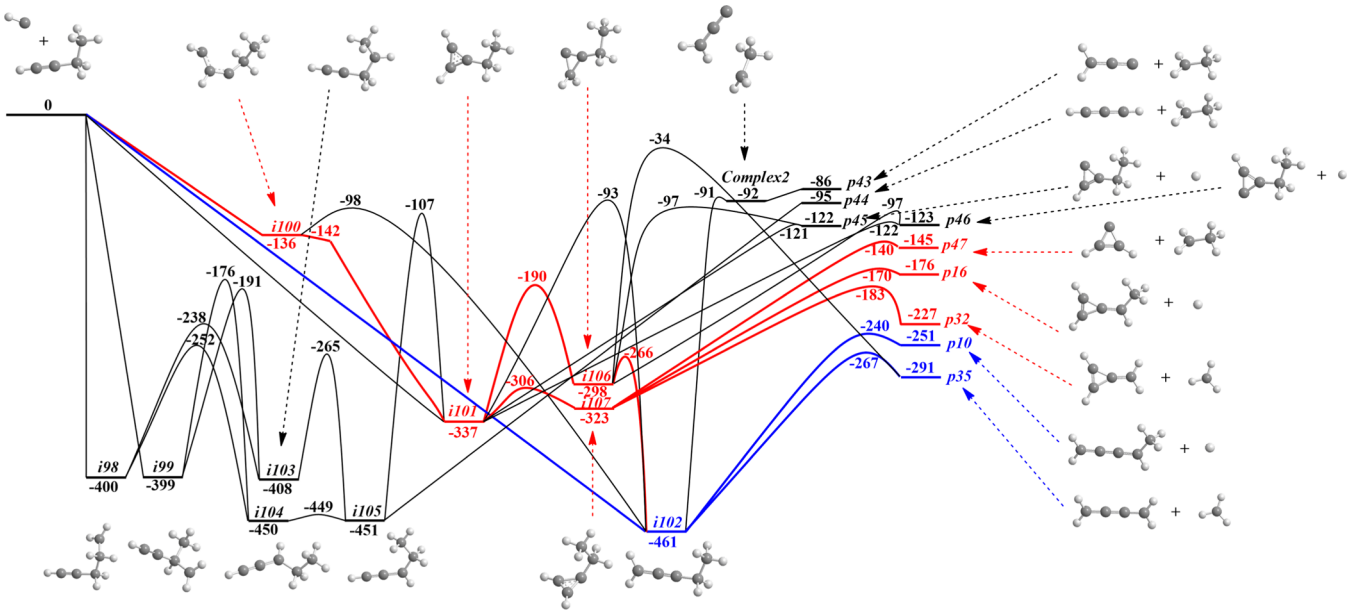

Figure 1. Potential energy diagram for the CH + 1-butyne reaction calculated at the CCSD(T)-F12/*cc*-pVTZ-f12//ωB97X-D/6-311G(d,p) + ZPE[ωB97X-D/6-311G(d,p)] level of theory including reaction channels leading to products **p10**, **p16**, **p32**, **p35**, and **p43**−**p47**. All relative energies are given in kJ mol^{-1}.

indicating that the formation mechanisms of C_5 hydrocarbon species are still far from being fully understood.

Among the C_5H_x PESs involved in the aforementioned reactions, the C_5H_7 surface is likely the most intricate one, owing to the high degree of unsaturation of the carbon atoms and a medium number of hydrogen atoms between 0 and 12 (as in fully saturated pentane C_5H_{12}), which results in a combinatorial growth of possible C_5 skeletons with various positions of double and triple bonds and ring structures and a variety of different placements of seven H atoms on five carbons. In addition to its complexity, the C_5H_7 PES is important both for combustion and astrochemistry because it can be accessed by a number of chemical reactions between hydrocarbon molecules and radicals present in flames and/or the interstellar medium including CH + C_4H_6, CH_2 + C_4H_5, CH_3 + C_4H_4, CH_4 + C_4H_3, C_2H + C_3H_6, C_2H_2 + C_3H_5, C_2H_3 + C_3H_4, C_2H_4 + C_3H_3, and others. In recent studies, we began our detailed investigation of the C_5H_7 surface by carrying out combined experimental crossed molecular beam and theoretical electronic structure/kinetic studies of the reactions of the methylidyne radical CH($X^2\Pi$) with two C_4H_6 isomers, 1,3- and 1,2-butadienes.[24,25] For instance, we found that the methylidyne radical may add barrierlessly to the terminal carbon atom and/or carbon−carbon double bond of 1,3-butadiene, leading to doublet C_5H_7 collision complexes, which, according to the experimental data, undergo non-statistical unimolecular decomposition *via* H atom emission, yielding the cyclic *cis*- and *trans*-3-vinyl-cyclopropene products, whereas the statistically favored product is cyclopentadiene. The CH + 1,2-butadiene reaction has been shown to proceed also through the barrierless addition of the methylidyne radical to the carbon−carbon double bonds of 1,2-butadiene, leading to C_5H_7 collision adducts, which lose atomic hydrogen to produce at least the cyclic 1-vinyl-cyclopropene, 1-methyl-3-methylenecyclopropene, and 1,2-*bis*(methylene) cyclopropane C_5H_6 isomers. The experimentally observed products were non-statistical, whereas statistical theoretical calculations predicted vinylacetylene plus methyl radical or (*Z*)/(*E*)-3-penten-1-yne + H to be the most likely products depending on whether CH adds to the terminal or central C═C double bond of 1,2-butadiene. Because the reactions of CH with 1,3- and 1,2-butadienes have been shown to be barrierless, exoergic, and with all transition states located below the energy of the initial reactants, the observed C_5H_6 products were predicted to be accessed even in low-temperature environments, such as in hydrocarbon-rich atmospheres of planets and cold molecular clouds such as TMC-1 and hence were proposed as viable targets for the astronomical search.

In the present work, we expand our theoretical exploration of the C_5H_7 PES by considering the reaction of methylidyne with 1-butyne. We show that the CH + 1-butyne reaction is also feasible at low temperatures but, contrary to the reactions with the butadienes, does not result in molecular growth processes of the carbon skeleton to C_5 species; instead this reaction generates less saturated C_4H_4 isomers (methylenecyclopropene, vinylacetylene, and 1,2,3-butatriene) along with smaller C_2 and C_3 hydrocarbons such as methyl, ethyl, and propargyl radicals, ethylene, and cyclopropenylidene.

■ COMPUTATIONAL METHODS

Geometry optimization of different species on the C_5H_7 PES related to the CH + 1-butyne reaction was carried out at the long-range corrected hybrid density functional ωB97X-D level of theory[26] with the 6-311G(d,p) basis set. Then, vibrational frequencies corresponding to each stationary structure were calculated at the same ωB97X-D/6-311G(d,p) level to obtain zero-point vibrational energy corrections (ZPE) and for further rate constant computation. Single-point energies for all optimized structures were refined applying the explicitly correlated couple cluster technique with single and double excitations and perturbative treatment of triple excitations CCSD(T)-F12[27,28] along with Dunning's correlation-consistent *cc*-pVTZ-f12 basis set.[29] The CCSD(T)-F12/*cc*-pVTZ-f12//ωB97X-D/6-311G(d,p) + ZPE[ωB97X-D/6-311G(d,p)] combination is expected to provide accuracy in relative

https://doi.org/10.1021/acs.jpca.1c07519
J. Phys. Chem. A 2021, 125, 9536−9547

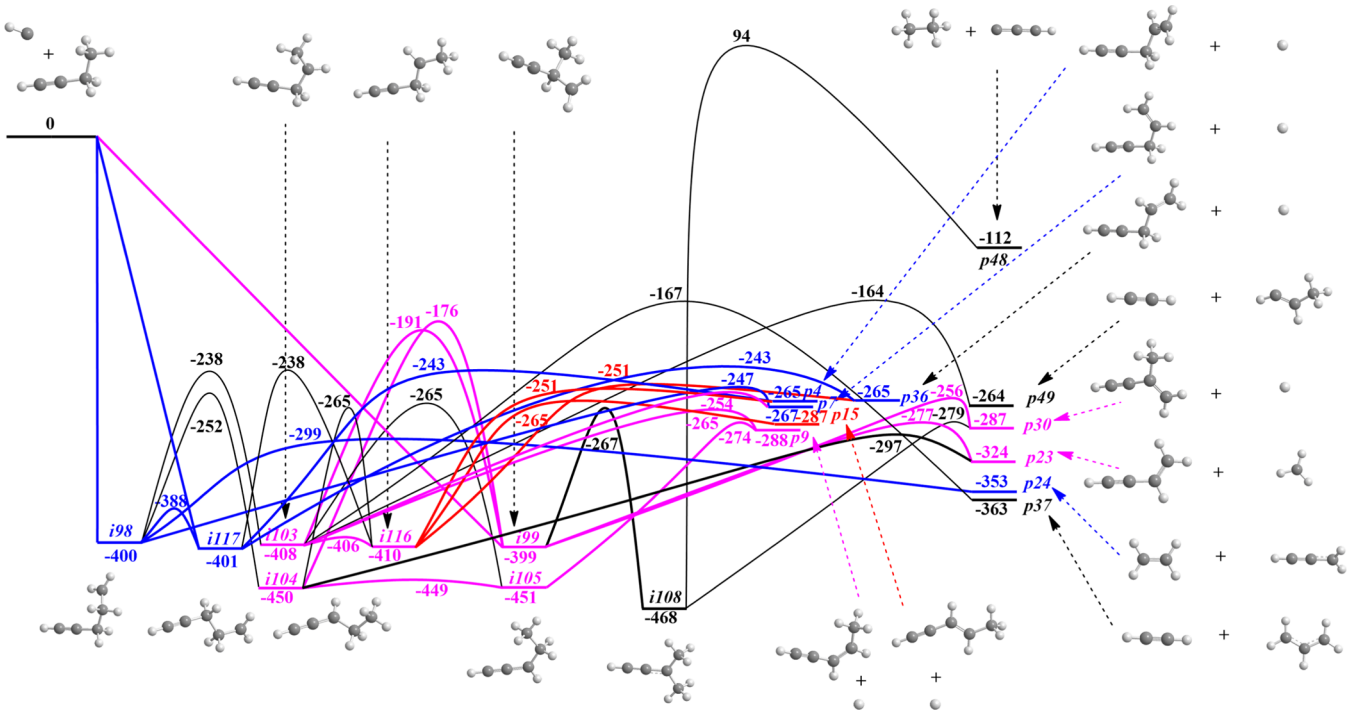

Figure 2. Potential energy diagram for the CH + 1-butyne reaction calculated at the CCSD(T)-F12/*cc*-pVTZ-f12//ωB97X-D/6-311G(d,p) + ZPE[ωB97X-D/6-311G(d,p)] level of theory including reaction channels to **p4**, **p7**, **p9**, **p15**, **p23**, **p24**, **p30**, **p36**, **p37**, **p48**, and **p49**. All relative energies are given in kJ mol^{-1}.

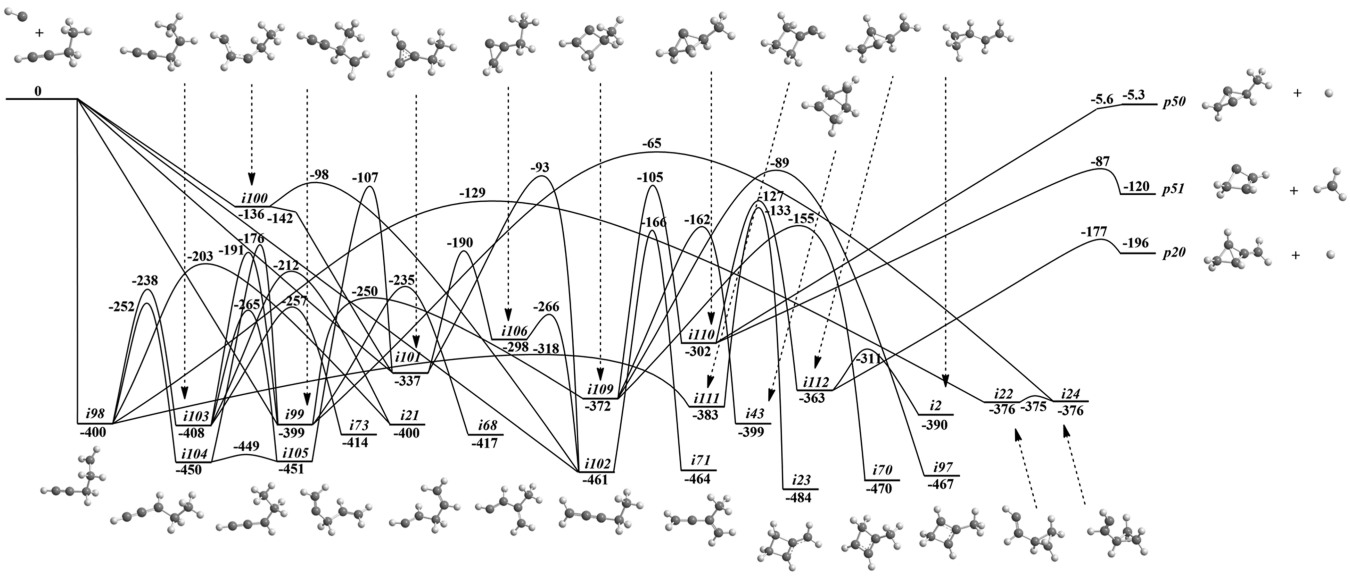

Figure 3. Potential energy diagram for the CH + 1-butyne reaction calculated at the CCSD(T)-F12/*cc*-pVTZ-f12//ωB97X-D/6-311G(d,p) + ZPE[ωB97X-D/6-311G(d,p)] level of theory including reaction channels toward products **p20**, **p50**, and **p51** and intermediates **i2**, **i21**−**i24**, **i43**, **i68**, **i70**, **i71**, **i73**, and **i97**. All relative energies are given in kJ mol^{-1}.

energies within 4 kJ mol^{-1} or even better.[30] The electronic structure calculations were performed using the GAUSSIAN 09[31] and MOLPRO 2010[32] quantum chemistry software packages.

Energy-dependent rate constants of all unimolecular reaction steps occurring on the C_5H_7 surface after the initial bimolecular association stage were computed utilizing the Rice−Ramsperger−Kassel−Marcus (RRKM) approach.[33−35] The internal energy for all the C_5H_7 isomers and products was supposed to be equal to the sum of the collision and chemical activation energies, where the latter is obtained as a negative of the relative energy of each species with regard to the separated CH + 1-butyne reactants. The rate constants were evaluated as functions of the internal energy of the individual intermediate or transition state by making use of our in-house code Unimol.[36] In order to reproduce the crossed molecular beam conditions emulating those in outer space, the calculations were performed at the zero-pressure limit. Note that a detailed description of the conditions of crossed molecular beam experiments is provided in numerous previous

https://doi.org/10.1021/acs.jpca.1c07519
J. Phys. Chem. A 2021, 125, 9536−9547

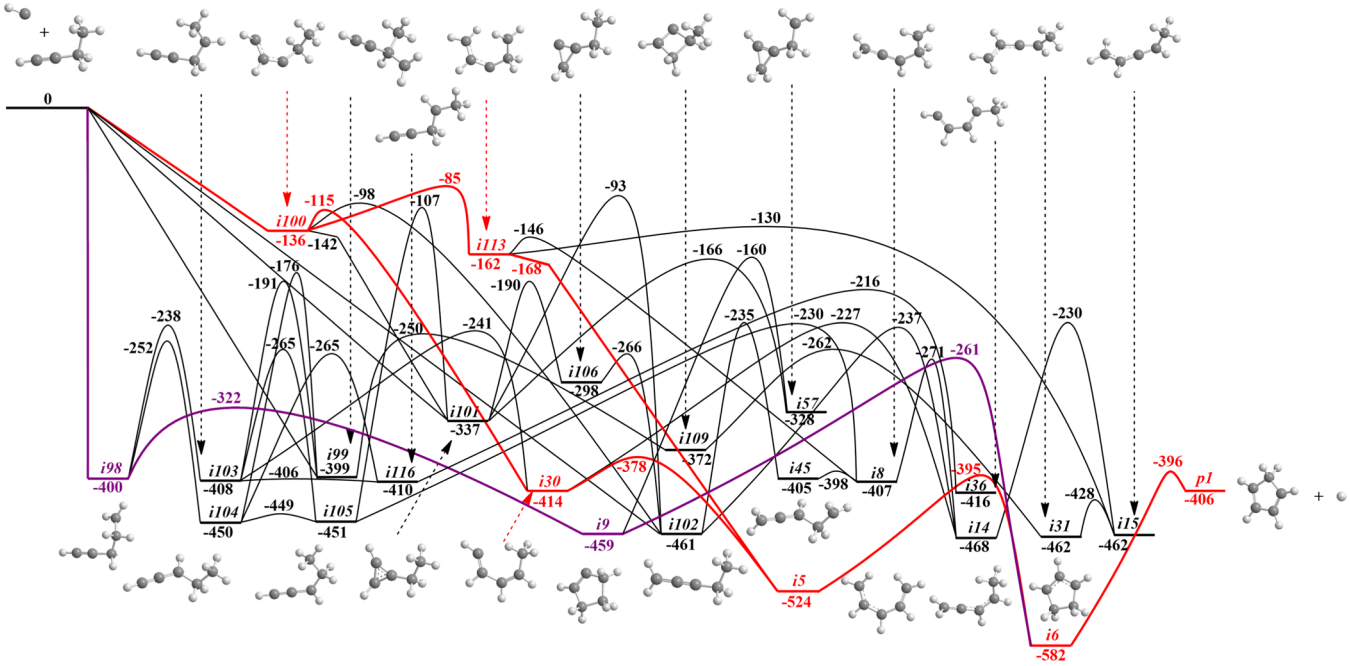

Figure 4. Potential energy diagram for the CH + 1-butyne reaction calculated at the CCSD(T)-F12/*cc*-pVTZ-f12//ωB97X-D/6-311G(d,p) + ZPE[ωB97X-D/6-311G(d,p)] level of theory including reaction channels leading to product **p1** and **i5**, **i6**, **i8**, **i9**, **i14**, **i15**, **i30**, **i31**, **i36**, **i45**, and **i57** intermediates. All relative energies are given in kJ mol^{-1}.

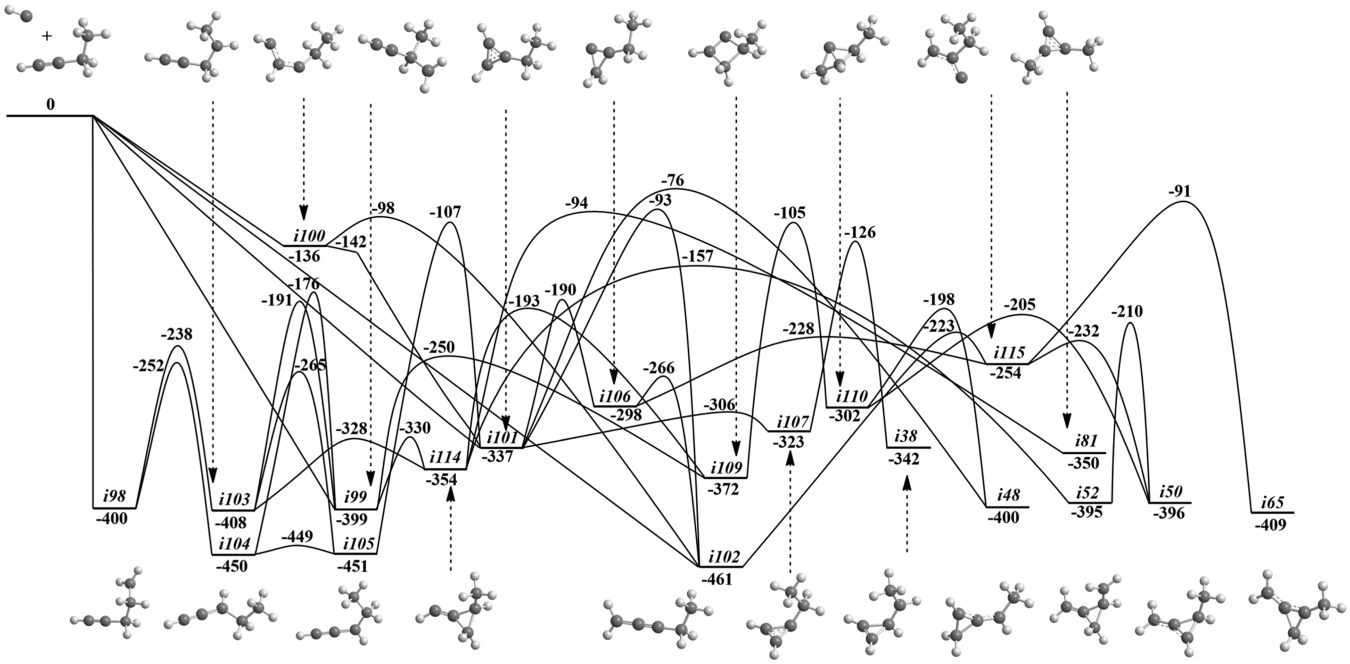

Figure 5. Potential energy diagram for the CH + 1-butyne reaction calculated at the CCSD(T)-F12/*cc*-pVTZ-f12//ωB97X-D/6-311G(d,p) + ZPE[ωB97X-D/6-311G(d,p)] level of theory including reaction channels leading to intermediates **i38**, **i48**, **i50**, **i52**, **i65**, and **i81**. All relative energies are given in kJ mol^{-1}.

studies, in particular, in the recent publications on the CH + 1,3-/1,2-butadiene reactions.[24,25] Finally, RRKM rate constants were used to evaluate reaction product branching ratios within steady-state approximation.[36,37]

■ RESULTS AND DISCUSSION

Using the electronic structure and statistical calculations below, we uncover various mechanisms giving rise to diverse products of the CH + C_4H_6 reaction. The initial interaction between the reactants may occur *via* methylidyne addition to acetylenic carbon atoms or to the triple C≡C bond of 1-butyne and methylidyne insertion into various C−H bonds of the C_4H_6 molecule. The doublet C_5H_7 PES was investigated gradually and systematically, in continuation of our previous CH + 1,3-/1,2-butadiene studies[24,25] and keeping the notation of intermediates and bimolecular products consistent with the previous works. Here, our calculations showed that the methylidyne radical plus 1-butyne system accesses 21 C_5H_7

https://doi.org/10.1021/acs.jpca.1c07519
J. Phys. Chem. A 2021, 125, 9536−9547

Table 1. Statistical Branching Ratios (%) for the Reaction of CH + 1-Butyne at a Collision Energy E_C of 20.6 kJ mol^{-1}[a]

		initial intermediate				
notation	name	i98/i117	i99	i100	i101	i102
p1	cyclopentadiene + H	0.1	0.4	8.5	0.1	0.2
p2	*trans*-1,2,4-pentatriene + H	0.0	0.1	1.3	0.0	0.2
p3	*cis*-1,2,4-pentatriene + H	0.3	0.1	1.5	0.0	0.4
p4	4-penten-1-yne + H	4.2	6.4	0.0	0.0	0.0
p5	1-vinylcyclopropene + H	0.0	0.0	0.1	0.1	0.0
p6	*cis*-3-vinylcyclopropene + H	0.0	0.0	0.0	0.0	0.0
p7	4-penten-1-yne + H (a conformer of **p4**)	4.2	4.8	0.1	0.0	0.0
p8	1-penten-3-yne + H	0.0	0.0	0.1	0.0	0.0
p9	(*Z*)-3-penten-1-yne + H	0.6	6.1	4.8	0.1	0.8
p10	1,2,3-pentatriene + H	0.0	0.0	1.2	0.8	11.2
p11	*trans*-3-vinylcyclopropene + H	0.0	0.0	0.0	0.0	0.0
p12	1-methyl-1,3-cyclobutadiene + H	0.0	0.0	0.0	0.0	0.0
p13	3-methylenecyclobutene + H	0.0	0.0	0.0	0.0	0.0
p14	cyclopropylacetylene + H	0.1	0.0	0.0	0.0	0.1
p15	(*E*)-3-penten-1-yne + H	0.6	7.3	2.1	0.1	0.9
p16	3-ethylidene-cyclopropene + H	0.0	0.0	5.8	7.6	0.0
p17	bicyclo[2.1.0]pent-1(4)-ene + H	0.0	0.0	0.0	0.0	0.0
p18	cyclopropene + C_2H_3 radical	0.0	0.0	0.0	0.0	0.0
p19	cyclobutadiene + CH_3 radical	0.0	0.0	0.0	0.0	0.0
p20	2-methylenebicyclo[1.1.0]butane + H	0.0	0.0	0.0	0.0	0.0
p21	bicyclo[2.1.0]pent-2-ene + H	0.0	0.0	0.0	0.0	0.0
p22	acetylene + *c*-CCH_2CH_2 radical	0.0	0.0	0.0	0.0	0.0
p23	vinylacetylene + CH_3 radical	1.2	55.2	0.3	0.1	0.0
p24	ethylene + CH_2CCH (propargyl) radical	84.3	1.1	0.4	0.2	2.2
p25	spiro[2.2]pent-1-ene + H	0.0	0.0	0.0	0.0	0.0
p26	1-vinyl-cyclopropene + H (a conformer of p5)	0.0	0.0	0.1	0.1	0.0
p27	ethenylidenecyclopropane + H	0.0	0.0	0.0	0.0	0.0
p28	1-methyl-3-methylenecyclopropene + H	0.0	0.0	0.0	0.0	0.0
p29	1,2-*bis*(methylene)cyclopropane + H	0.0	0.0	0.0	0.0	0.0
p30	2-methyl-1-buten-3-yne + H	0.0	10.6	0.0	0.0	0.0
p31	ethylene + *c*-$CCHCH_2$ radical	0.0	0.0	0.1	0.2	0.0
p32	methylenecyclopropene + CH_3 radical	0.0	0.0	41.4	54.7	0.0
p33	allene + C_2H_3 radical	0.0	0.4	0.1	0.0	0.0
p34	acetylene + CH_3CCH_2 radical	0.0	0.6	0.0	0.0	0.0
p35	1,2,3-butatriene + CH_3 radical	0.0	0.0	9.2	5.8	84.0
p36	4-penten-1-yne + H (a conformer of p4)	4.2	6.3	0.0	0.0	0.0
p37	acetylene + CH_2CHCH_2 (allyl) radical	0.2	0.5	0.0	0.0	0.0
p38	propyne + C_2H_3 radical	0.0	0.0	0.1	0.0	0.0
p39	methylcyclopropenylidene + CH_3 radical	0.0	0.0	0.0	0.0	0.0
p40	dimethylcyclopropenylidene + H	0.0	0.0	0.0	0.0	0.0
p41-m1	singlet dimethylpropargylene + H	0.0	0.0	0.0	0.0	0.0
p41-m3	triplet dimethylpropargylene + H	0.0	0.0	0.0	0.0	0.0
p42	ethylene + $CCCH_3$ radical	0.0	0.0	0.0	0.0	0.0
p43	vinylidenecarbene + C_2H_5 radical	0.0	0.0	0.0	0.0	0.0
p44	propargylene + C_2H_5 radical	0.0	0.0	0.0	0.0	0.0
p45	ethylcyclopropenylidene + H	0.0	0.0	1.1	1.4	0.0
p46	ethylcyclopropenylidene + H (a conformer of p45)	0.0	0.0	1.1	1.5	0.0
p47	cyclopropenylidene + C_2H_5 radical	0.0	0.0	20.6	27.2	0.0
p48	ethane + CCCH radical	0.0	0.0	0.0	0.0	0.0
p49	acetylene + CH_3CHCH radical	0.0	0.1	0.0	0.0	0.0
p50	2-methylbicyclo[1.1.0]but-1(3)-ene + H	0.0	0.0	0.0	0.0	0.0
p51	cyclobutenylidene + CH_3 radical	0.0	0.0	0.0	0.0	0.0

[a]A value for the collision energy was chosen to be similar to that in the recent crossed molecular beam studies of the CH reactions with 1,3- and 1,2-butadienes (refs 24 and 25).

intermediates (**i98**−**i117** and **complex2**) and 92 transition states, leading to the hydrogen atom emission C_5H_6 products (**p1**, **p4**, **p7**, **p9**, **p10**, **p15**, **p16**, **p20**, **p30**, **p36**, **p45**, **p46**, and **p50**), methyl radical elimination C_4H_4 products (**p23**, **p32**, **p35**, and **p51**), ethyl radical loss C_3H_2 products (**p43**, **p44**, and **p47**), linear C_3H radical emission C_2H_6 product (**p48**), propargyl radical loss C_2H_4 product (**p24**), and allyl CH_2CHCH_2 and 3-propenyl CH_3CHCH radical loss C_2H_2

https://doi.org/10.1021/acs.jpca.1c07519
J. Phys. Chem. A 2021, 125, 9536−9547

products (**p37** and **p49**, respectively) (Figures 1, 2, 3, 4, 5; Table 1). Because some pathways of the CH + 1-butyne reaction eventually access the intermediates considered earlier, in the studies of CH reactions with the other C_4H_6 isomers,[24,25] we occasionally stop the PES presentation and our discussion at the common intermediates. Moreover, as will be seen (*vide infra*) from the calculations of product branching ratios, the prevalent reaction products would be formed through relatively short pathways, which do not involve the common intermediates. The presentation of the overall C_5H_7 PES considered in the present work is split into five figures to simplify the discussion on the reaction mechanism:

(1) Reaction channels leading to products **p10**, **p16**, **p32**, **p35**, and **p43**−**p47** formed *via* methylidyne radical addition to the terminal carbon atom and the triple C≡C bond of the ethynyl fragment and insertion into terminal C−H bonds of the ethyl or ethynyl moieties, and non-terminal C−H bonds of the ethyl fragment in the 1-butyne molecule *via* intermediates **i98**−**i107** and **complex2** (Figure 1);

(2) Channels to **p4**, **p7**, **p9**, **p15**, **p23**, **p24**, **p30**, **p36**, **p37**, **p48**, and **p49** resulting from methylidyne radical insertion into terminal and non-terminal C−H bonds of the C_2H_5 fragment of 1-butyne including intermediates **i98**, **i99**, **i103**−**i105**, **i108**, **i116**, and **i117** (Figure 2);

(3) Pathways originating from the same initial channels as in item 1 toward products **p20**, **p50**, and **p51** and intermediates **i2**, **i21**−**i24**, **i43**, **i68**, **i70**, **i71**, **i73**, and **i97** studied earlier for CH reactions with 1,3-butadiene and 1,2-butadiene through **i98**−**i106** and **i109**−**i112** (Figure 3);

(4) Product channels leading to **p1** as well as to **i5**, **i6**, **i8**, **i9**, **i14**, **i15**, **i30**, **i31**, **i36**, **i45**, and **i57** intermediates of CH + 1,3-butadiene/1,2-butadiene reactions stemming from the same initial pathways as in item 1 and involving **i98**−**i106**, **i109**, **i113**, and **i116** (Figure 4);

(5) Pathways to intermediates **i38**, **i48**, **i50**, **i52**, **i65**, and **i81** produced by the same entrance channels as in item 1 *via* **i98**−**i107**, **i109**, **i110**, **i114**, and **i115** (Figure 5).

In the following sections, we briefly describe the most significant reaction pathways depicted in these Figures.

Product Channels p10, p16, p32, p35, and p43−p47. As seen in Figure 1, the methylidyne radical may add barrierlessly to the terminal carbon atom of 1-butyne and to the triple C≡C bond and additionally may insert into terminal C−H bonds of the ethyl or ethynyl fragments and non-terminal C−H bonds of the ethyl moiety of 1-butyne, forming the initial adducts **i100**, **i101**, and **i98** or **i102** and **i99**, respectively. From **i98**, 1,2- and 1,3-hydrogen shifts from the non-terminal CH_2 group to the adjacent terminal CH_2 fragment and from the non-terminal CH_2 group of the central carbon to the terminal CH_2 fragment lead to **i103** and **i104** *via* high barriers of 162 and 148 kJ mol^{-1} above **i98**, respectively. Intermediates **i103** and **i104**, for their part, are connected to another initial intermediate **i99** by the ethynyl and methyl group migrations between CH and CH_2 through higher barriers of 208 and 223 kJ mol^{-1} above **i99**, respectively. The C_2H_5 moiety rotation in **i104** results in **i105** *via* a low barrier, with the corresponding transition state lying 1 kJ mol^{-1} above **i104**. Then, hydrogen migration from the non-terminal CH group to the adjacent bare carbon atom along with a three-member ring closure in **i105** can give rise to the adduct **i101**. The intermediates **i103** and **i105** are linked *via* a 1,2-H migration from the CH_2 fragment to the adjacent CH group in **i103** with a barrier of 143 kJ mol^{-1} relative to **i103**. From **i105**, the ethyl fragment loss produces the product **p44**—triplet propargylene C_3H_2, without an exit barrier.

It is important to note that the initial adduct **i100** is found to be metastable with respect to its three-member ring closure forming **i101**. A tiny barrier of 0.2 kJ mol^{-1} between **i100** and **i101** is located at the ωB97X-D/6-311G(d,p) level of theory, but after the energy of the **i100**-**i101** transition state is refined at the CCSD(T)-F12/*cc*-pVTZ-f12 level, it slides slightly below that of the adduct **i100**. Hydrogen migration from the non-terminal CH moiety to the terminal CH moiety in **i100** connects it with **i102** *via* a barrier of 38 kJ mol^{-1}. An alternative way of reaching **i102** is the hydrogen shift from one CH group to another in the *c*-CCHCH moiety of **i101** resulting in **i106**, with the subsequent ring opening in **i106** leading to **i102**. A pair of the products **p45** and **p46** (ethyl-substituted cyclopropenylidenes) are accessible either *via* the atomic hydrogen elimination from both CH groups in the three-member ring of **i101** *via* loose exit transition states located only 1 kJ mol^{-1} above the separated products or through a hydrogen loss from the CH_2 group of the *c*-$CCCH_2$ fragment of **i106** *via* tight exit transition states residing 25 and 26 kJ mol^{-1} above the separated products, respectively.

i101 can isomerize to **i107** *via* a fairly low barrier of 31 kJ mol^{-1}. A hydrogen loss from the CH_2 group in **i107** leads to the product **p16** through a loose exit transition state lying 6 kJ mol^{-1} above the separated products, whereas the C_2H_5 and CH_3 eliminations from **i107** result in the products **p32** (methylenecyclopropene) and **p47** (cyclopropenylidene) through the tight and loose exit transition state located 44 and 5 kJ mol^{-1} above the separated products, respectively. **i102** can also form three different products **p10** (1,2,3-pentatriene), **p35** (1,2,3-butatriene), and **p43** (vinylidenecarbene), involving an atomic hydrogen loss from the non-terminal CH_2 moiety *via* a loose exit transition state residing 11 kJ mol^{-1} above the separated products for **p10** and the CH_3 and C_2H_5 emissions for **p35** and **p43**, respectively. It is interesting to note that on the path of **i102** decomposition to **p43**, a weak product **complex2** forms first *via* a barrier of 1 kJ mol^{-1} above itself and then **complex2** dissociates to **p43** with addition of extra 5 kJ mol^{-1}. The product **p35** is accessed by the CH_3 loss *via* a tight exit transition state lying 24 kJ mol^{-1} above the separated products. Besides, the product **p35** may be formed by the CH_3 loss along with the three-member ring opening in **i106** *via* a very high barrier of 257 kJ mol^{-1} above the separated products.

Summarizing, the product **p44** can be formed *via* pathway 1 by the C_2H_5 moiety loss from **i105**, in case the methylidyne radical inserts into terminal or non-terminal C−H bonds of the C_2H_5 fragment. The products **p45** and **p46** may be accessed *via* pathway 2 by the hydrogen emission from CH groups of the three-member ring in **i101** or from the CH_2 group of the *c*-$CCCH_2$ moiety in **i106** if the CH radical adds to the terminal carbon or the triple C≡C bond or inserts into the terminal C−H bond of the C_2H fragment. The products **p16**, **p32**, and **p47** can be reached through pathway 3 by an H loss from the non-terminal CH_2 group and CH_3 and C_2H_5 emissions in **i107**, respectively, *via* the same entrance channels as in pathway 2. Products **p10**, **p35**, and **p43** may be produced *via* pathway 4 by an H loss from the non-terminal CH_2 group and CH_3 and C_2H_5 eliminations from **i102**, respectively. Less favorable

https://doi.org/10.1021/acs.jpca.1c07519
J. Phys. Chem. A 2021, 125, 9536−9547

pathways (1a—4a) leading to the same products as (1−4), respectively, but featuring higher barriers, are also specified below in order to take into account all initial adducts **i98**−**i102**:

$$CH + CH_3CH_2CCH \rightarrow [\mathbf{i98}/\mathbf{i99} \rightarrow \mathbf{i103}/\mathbf{i104}] \rightarrow \mathbf{i105} \rightarrow \mathbf{p44} + C_2H_5 \quad (1)$$

$$CH + CH_3CH_2CCH \rightarrow [\mathbf{i100}]/[\mathbf{i102}]/[\mathbf{i102} \rightarrow \mathbf{i106}] \rightarrow \mathbf{i101} \rightarrow \mathbf{i105} \rightarrow \mathbf{p44} + C_2H_5 \quad (1a)$$

$$CH + CH_3CH_2CCH \rightarrow [\mathbf{i101}]/[\mathbf{i100} \rightarrow \mathbf{i101}]/[\mathbf{i100} \rightarrow \mathbf{i101} \rightarrow \mathbf{i106}]/[\mathbf{i102} \rightarrow \mathbf{i106}]/[\mathbf{i102} \rightarrow \mathbf{i106} \rightarrow \mathbf{i101}] \rightarrow \mathbf{p45} + H/\mathbf{p46} + H \quad (2)$$

$$CH + CH_3CH_2CCH \rightarrow [\mathbf{i98}/\mathbf{i99} \rightarrow \mathbf{i103}/\mathbf{i104} \rightarrow \mathbf{i105}]/[\mathbf{i102}] \rightarrow \mathbf{i101} \rightarrow \mathbf{p45} + H/\mathbf{p46} + H \quad (2a)$$

$$CH + CH_3CH_2CCH \rightarrow [\mathbf{i101}]/[\mathbf{i100} \rightarrow \mathbf{i101}]/[\mathbf{i102} \rightarrow \mathbf{i106} \rightarrow \mathbf{i101}] \rightarrow \mathbf{i107} \rightarrow \mathbf{p16} + H/\mathbf{p32} + CH_3/\mathbf{p47} + C_2H_5 \quad (3)$$

$$CH + CH_3CH_2CCH \rightarrow [\mathbf{i98}/\mathbf{i99} \rightarrow \mathbf{i103}/\mathbf{i104} \rightarrow \mathbf{i105}]/[\mathbf{i102}] \rightarrow \mathbf{i101} \rightarrow \mathbf{i107} \rightarrow \mathbf{p16} + H/\mathbf{p32} + CH_3/\mathbf{p47} + C_2H_5 \quad (3a)$$

$$CH + CH_3CH_2CCH \rightarrow [\mathbf{i102}]/[\mathbf{i100} \rightarrow \mathbf{i102}]/[\mathbf{i100} \rightarrow \mathbf{i101} \rightarrow \mathbf{i106} \rightarrow \mathbf{i102}] \rightarrow \mathbf{p10} + H/\mathbf{p35} + CH_3/[\text{complex2} \rightarrow \mathbf{p43} + C_2H_5] \quad (4)$$

$$CH + CH_3CH_2CCH \rightarrow [\mathbf{i98}/\mathbf{i99} \rightarrow \mathbf{i103}/\mathbf{i104} \rightarrow \mathbf{i105}] \rightarrow [\mathbf{i101}]/[\mathbf{i101} \rightarrow \mathbf{i106}] \rightarrow \mathbf{i102} \rightarrow \mathbf{p10} + H/\mathbf{p35} + CH_3/[\text{complex2} \rightarrow \mathbf{p43} + C_2H_5] \quad (4a)$$

Product channels p4, p7, p9, p15, p23, p24, p30, p36, p37, p48, and p49. As shown in Figure 2, methyl radical emission from **i99** and **i104** yields the vinylacetylene product **p23** *via* transition states lying 47 and 27 kJ mol^{-1} above the separated products (channels 5, 5a). The intermediate **i108** is connected with the initial adduct **i99** by the hydrogen migration from the non-terminal CH group to the terminal CH_2 moiety of **i99** proceeding through a high barrier of 132 kJ mol^{-1} above **i99**. A hydrogen loss from CH_3 groups in **i99** and **i108** gives rise to **p30** (2-methyl-1-buten-3-yne) *via* tight and loose exit transition states respectively located 31 and 8 kJ mol^{-1} above the separated products (channels 6, 6a). An atomic hydrogen emission from the middle non-terminal CH_2 group of the $CH_2CH_2CH_2$ moiety in **i98** and from the terminal CH_3 group in **i103** yields the product **p7** (4-penten-1-yne) *via* exit transition states residing 20 and 13 kJ mol^{-1} above the separated products, respectively (channels 7, 7a). The intermediate **i98** may decay into the propargyl radical plus ethylene (**p24**, channels 8, 8a). The product **p9** [(*Z*)-3-penten-1-yne] might be accessed by an H loss from the non-terminal CH_2 fragments in **i103** and **i105** *via* exit transition states lying 23 and 14 kJ mol^{-1} above the separated products, respectively (channels 9, 9a). **i103** can isomerize to **i116** *via* a very low barrier of 2 kJ mol^{-1} above **i103** by rotation of the $CHCH_3$ fragment around the CH−CH_2 bond. Similarly, a low-lying transition state of 12 kJ mol^{-1} above **i98** connects rotational conformers **i98** and **i117**. Alternatively, a high barrier of 163 kJ mol^{-1} corresponding to an H shift from the terminal CH_3 group to the adjacent CH_2 moiety in **i116** separates the **i116** and **i117** intermediates. Three products **p4**, **p15**, and **p36** representing various conformers of 4-penten-1-yne may be formed by a hydrogen elimination from the terminal CH_3 group in **i116** or from the non-terminal CH_2 group of the terminal CH_2CH_2 moiety in **i117** (**p4** and **p36**) and from the non-terminal CH_2 fragment in **i116** (**p15**) *via* transition states located 14 or 22 kJ mol^{-1} above **p4** and **p36** and 22 kJ mol^{-1} above **p15** (channels 10, 10a). The intermediate **i108** can in principle also decompose to **p48** (ethane + linear C_3H) but the corresponding transition state residing 94 kJ mol^{-1} above the initial reactants makes this channel rather non-competitive (channels 11, 11a). The isomer **i103** can emit the CCH fragment, whereby this fragment while splitting apart may capture a hydrogen atom either from the CH_2 or CH_3 groups of the CH_2CHCH_3 moiety, producing as a result acetylene + C_3H_5 radicals **p37** (allyl) or **p49** (3-propenyl) *via* very high barriers (channels 12, 12a).

$$CH + CH_3CH_2CCH \rightarrow [\mathbf{i99}]/[\mathbf{i98}/\mathbf{i99} \rightarrow \mathbf{i104}] \rightarrow \mathbf{p23} + CH_3 \quad (5)$$

$$CH + CH_3CH_2CCH \rightarrow [\mathbf{i100}/\mathbf{i102} \rightarrow \mathbf{i101i} \rightarrow 105\mathbf{i} \rightarrow 104]/[\mathbf{i102} \rightarrow \mathbf{i106} \rightarrow \mathbf{i101} \rightarrow \mathbf{i105} \rightarrow \mathbf{i104}]/[\mathbf{i98} \rightarrow \mathbf{i103}/\mathbf{i104} \rightarrow \mathbf{i99}] \rightarrow \mathbf{p23} + CH_3 \quad (5a)$$

$$CH + CH_3CH_2CCH \rightarrow [\mathbf{i99}]/[\mathbf{i99} \rightarrow \mathbf{i108}]/[\mathbf{i98} \rightarrow \mathbf{i103}/\mathbf{i104} \rightarrow \mathbf{i99}] \rightarrow \mathbf{p30} + H \quad (6)$$

$$CH + CH_3CH_2CCH \rightarrow [\mathbf{i101}]/[\mathbf{i100}/\mathbf{i102} \rightarrow \mathbf{i101}]/[\mathbf{i102} \rightarrow \mathbf{i106} \rightarrow \mathbf{i101}] \rightarrow \mathbf{i105} \rightarrow [\mathbf{i103}/\mathbf{i104}] \rightarrow \mathbf{i99} \rightarrow \mathbf{p30} + H \quad (6a)$$

$$CH + CH_3CH_2CCH \rightarrow [\mathbf{i98}]/[\mathbf{i98}/\mathbf{i99} \rightarrow \mathbf{i103}] \rightarrow \mathbf{p7} + H \quad (7)$$

$$CH + CH_3CH_2CCH \rightarrow [\mathbf{i101}]/[\mathbf{i100}/\mathbf{i102} \rightarrow \mathbf{i101}]/[\mathbf{i102} \rightarrow \mathbf{i106} \rightarrow \mathbf{i101}] \rightarrow \mathbf{i105} \rightarrow [\mathbf{i103}]/[\mathbf{i103}/\mathbf{i104} \rightarrow \mathbf{i98}] \rightarrow \mathbf{p7} + H \quad (7a)$$

$$CH + CH_3CH_2CCH \rightarrow [\mathbf{i98}]/[\mathbf{i99} \rightarrow \mathbf{i103}/\mathbf{i104} \rightarrow \mathbf{i98}] \rightarrow \mathbf{p24} + CH_2CCH \quad (8)$$

$$CH + CH_3CH_2CCH \rightarrow [\mathbf{i100}]/[\mathbf{i102}]/[\mathbf{i102} \rightarrow \mathbf{i106}] \rightarrow \mathbf{i101} \rightarrow \mathbf{i105} \rightarrow [\mathbf{i103}/\mathbf{i104}] \rightarrow \mathbf{i98} \rightarrow \mathbf{p24} + CH_2CCH \quad (8a)$$

https://doi.org/10.1021/acs.jpca.1c07519
J. Phys. Chem. A 2021, 125, 9536−9547

$$CH + CH_3CH_2CCH \rightarrow [\mathbf{i98}/\mathbf{i99} \rightarrow \mathbf{i103}]/[\mathbf{i98}/\mathbf{i99} \rightarrow \mathbf{i103}/\mathbf{i104} \rightarrow \mathbf{i105}]/[\mathbf{i101} \rightarrow \mathbf{i105}] \rightarrow \mathbf{p9} + H \quad (9)$$

$$CH + CH_3CH_2CCH \rightarrow [\mathbf{i100}]/[\mathbf{i102}]/[\mathbf{i102} \rightarrow \mathbf{i106}] \rightarrow \mathbf{i101} \rightarrow [\mathbf{i105}]/[\mathbf{i105} \rightarrow \mathbf{i103}] \rightarrow \mathbf{p9} + H \quad (9a)$$

$$CH + CH_3CH_2CCH \rightarrow [\mathbf{i98}/\mathbf{i99} \rightarrow \mathbf{i103}/\mathbf{i104}] \rightarrow \mathbf{i116} \rightarrow \mathbf{p4}/\mathbf{p15}/\mathbf{p36} + H/[\mathbf{i117}]/[\mathbf{i98} \rightarrow \mathbf{i117}] \rightarrow \mathbf{p4}/\mathbf{p36} + H \quad (10)$$

$$CH + CH_3CH_2CCH \rightarrow [\mathbf{i100}]/[\mathbf{i102}]/[\mathbf{i102} \rightarrow \mathbf{i106}] \rightarrow \mathbf{i101} \rightarrow \mathbf{i105} \rightarrow \mathbf{i103} \rightarrow \mathbf{i116} \rightarrow \mathbf{p4}/\mathbf{p15}/\mathbf{p36} + H \quad (10a)$$

$$CH + CH_3CH_2CCH \rightarrow [\mathbf{i99}]/[\mathbf{i98} \rightarrow \mathbf{i103}/\mathbf{i104} \rightarrow \mathbf{i99}] \rightarrow \mathbf{i108} \rightarrow \mathbf{p48} + l\text{-}C_3H \quad (11)$$

$$CH + CH_3CH_2CCH \rightarrow [\mathbf{i100}]/[\mathbf{i102}]/[\mathbf{i102} \rightarrow \mathbf{i106}] \rightarrow \mathbf{i101} \rightarrow \mathbf{i105} \rightarrow [\mathbf{i103}/\mathbf{i104}] \rightarrow \mathbf{i99} \rightarrow \mathbf{i108} \rightarrow \mathbf{p48} + l\text{-}C_3H \quad (11a)$$

$$CH + CH_3CH_2CCH \rightarrow [\mathbf{i98}/\mathbf{i99}] \rightarrow \mathbf{i103} \rightarrow \mathbf{p37} + CH_2CHCH_2/\mathbf{p49} + CH_3CHCH \quad (12)$$

$$CH + CH_3CH_2CCH \rightarrow [\mathbf{i100}]/[\mathbf{i102}]/[\mathbf{i102} \rightarrow \mathbf{i106}] \rightarrow \mathbf{i101} \rightarrow \mathbf{i105} \rightarrow \mathbf{i103} \rightarrow \mathbf{p37} + CH_2CHCH_2/\mathbf{p49} + CH_3CHCH \quad (12a)$$

Product Channels p20, p50, and p51 and Pathways toward Intermediates i2, i21−i24, i43, i68, i70, i71, i73, and i97. As illustrated in Figure 3, hydrogen migration from the terminal CH_3 group to the other terminal CH group or to the bare carbon atom of the CCH fragment in **i103** connects it with **i73** or **i21**. As for **i99**, an atomic hydrogen shift from the non-terminal CH group to the adjacent bare carbon results in **i68**. Also, an H shift from the CH_2 group of the central carbon to the adjacent bare C atom in **i98** and from the terminal CH_3 group to the bare carbon of the ethynyl fragment in **i99** along with ring closure for each of the intermediates accesses **i22** and **i24** connected to one another *via* rotation of the CHCH moiety. A four-member ring closure in **i99** produces **i109**, which may further form **i43** by a hydrogen migration from the CH_3 group to a bare carbon atom in the ring with one more ring closure, or **i70** by the hydrogen shift from the CH group of the CH_3CH moiety to the bare carbon atom or **i97** by the CH_3 migration to the same bare carbon atom. The cyclic intermediate **i109** can move to **i110**, and the latter can decompose to two products **p50** (2-methylbicyclo[1.1.0]but-1(3)-ene) and **p51** (cyclobutenylidene) *via* the H loss from the CH group of the *c*-CH_2CCH moiety and CH_3 emission, respectively (pathways 13, 13a). It must be pointed out that even though the CCSD(T)-F12/*cc*-pVTZ-f12 refined energy of the transition state **i110-p50** is slightly lower than the separated products, there is a barrier of 3 kJ mol^{-1} above the separated products at the ωB97X-D/6-311G(d,p) level of theory. The CH_3 migration to the adjacent bare carbon atom in **i102** leads to **i71**. The isomer **i98** may form a cyclic species **i111** as well, and the next step would be an H shift from any of CH_2 groups, which are closest to the bare carbon atom in the four-member ring, to the CH moiety in **i111** giving rise to **i23**. A hydrogen migration from the CH_3 group to the bare carbon atom connects **i110** and **i112**. A C−C bond rupture in the four-member CH_2CHCH ring leads to **i2**, which contains a three-member ring and is an initial adduct of the CH + 1,3-butadiene reaction.[24] The product **p20** can be accessed from **i112** by H elimination from the CH group of the CH_2CH moiety *via* a tight exit transition state lying 19 kJ mol^{-1} above the separated products (pathways 14, 14a).

$$CH + CH_3CH_2CCH \rightarrow [\mathbf{i99}]/[\mathbf{i98} \rightarrow \mathbf{i103}/\mathbf{i104} \rightarrow \mathbf{i99}] \rightarrow \mathbf{i109} \rightarrow \mathbf{i110} \rightarrow \mathbf{p50} + H/\mathbf{p51} + CH_3 \quad (13)$$

$$CH + CH_3CH_2CCH \rightarrow [\mathbf{i100}]/[\mathbf{i102}]/[\mathbf{i102} \rightarrow \mathbf{i106}] \rightarrow \mathbf{i101} \rightarrow \mathbf{i105} \rightarrow [\mathbf{i103}/\mathbf{i104}] \rightarrow \mathbf{i99} \rightarrow \mathbf{i109} \rightarrow \mathbf{i110} \rightarrow \mathbf{p50} + H/\mathbf{p51} + CH_3 \quad (13a)$$

$$CH + CH_3CH_2CCH \rightarrow [\mathbf{i99}]/[\mathbf{i98} \rightarrow \mathbf{i103}/\mathbf{i104} \rightarrow \mathbf{i99}] \rightarrow \mathbf{i109} \rightarrow \mathbf{i110} \rightarrow \mathbf{i112} \rightarrow \mathbf{p20} + H \quad (14)$$

$$CH + CH_3CH_2CCH \rightarrow [\mathbf{i100}]/[\mathbf{i102}]/[\mathbf{i102} \rightarrow \mathbf{i106}] \rightarrow \mathbf{i101} \rightarrow \mathbf{i105} \rightarrow [\mathbf{i103}/\mathbf{i104}] \rightarrow \mathbf{i99} \rightarrow \mathbf{i109} \rightarrow \mathbf{i110} \rightarrow \mathbf{i112} \rightarrow \mathbf{p20} + H \quad (14a)$$

Note that the intermediates **i2**, **i21**−**i24**, **i43**, **i68**, **i70**, **i71**, and **i73** occurring on this part of the PES were encountered earlier in our studies of the CH +1,3-/1,2-butadiene reactions, and thus, their possible fates have been already discussed.[24,25] Nevertheless, the pathways leading from CH + 1-butyne through these C_5H_7 isomers do not appear to be competitive according to RRKM calculations (*vide infra*) due to the higher barriers involved.

Product Channel p1 and Pathways toward Intermediates i8, i9, i14, i15, i30, i31, i36, i45, and i57. In this section, we consider pathways leading to the most thermodynamically stable C_5H_6 product, cyclopentadiene **p1** (Figure 4). **p1** was predicted to be the preferable statistical product of the CH + 1,3-butadiene reaction according to our calculations but was not actually observed in the crossed beam experiments.[24] Considering the CH + 1-butyne reaction, a hydrogen shift from the terminal CH_3 group to the opposite terminal CH group in **i100** may lead to **i113**. The intermediate **i113** is metastable with respect to H migration from the non-terminal CH_2 group to the adjacent bare C atom. A 16 kJ mol^{-1} barrier for such migration was located at the ωB97X-D/6-311G(d,p) level of theory but the CCSD(T)-F12/*cc*-pVTZ-f12 refined energy of the transition state is below that of **i113**, indicating that its isomerization to **i5** is likely to be spontaneous. Next, **i5** can ring-close to **i6** and the latter gives rise to the most stable C_5H_6 product cyclopentadiene **p1** by an H loss from any of the two CH_2 groups (channel 15). Also, an H shift from the CH_2 group to the adjacent bare C atom in **i100** forms **i30**, and the latter can rearrange to **i5** by 1,5-H migration between the terminal CH_3 and CH groups. An alternative path to **i6** and thus to **p1** + H involves a five-member ring closure in **i98** to the intermediate **i9** followed by

https://doi.org/10.1021/acs.jpca.1c07519
J. Phys. Chem. A 2021, 125, 9536−9547

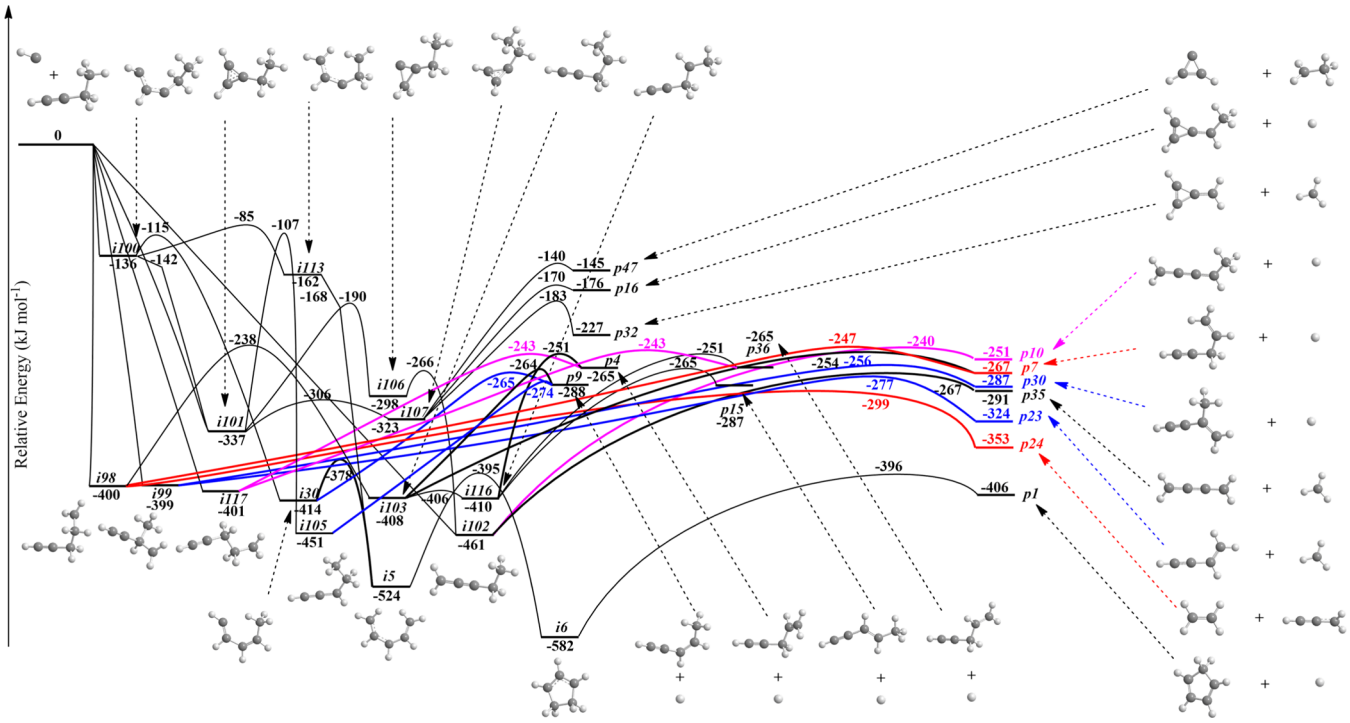

Figure 6. Potential energy diagram for the CH + 1-butyne reaction calculated at the CCSD(T)-F12/*cc*-pVTZ-f12//ωB97X-D/6-311G(d,p) + ZPE[ωB97X-D/6-311G(d,p)] level of theory including the most important reaction channels. All relative energies are given in kJ mol^{-1}.

H migration from CH_2 to the neighboring bare C atom in the ring. The **i5** intermediate can be also obtained from the initial adduct **i98** by a series of H migrations: first, 1,2-shift between two CH_2 groups to **i103**, second, 1,2-shift from CH_2 to the bare carbon to **i30**, and third, 1,5-shift between the two ends of the carbon chain *via* a relatively low barrier of 36 kJ mol^{-1} to **i5**. The four-member ring intermediate **i109** can be produced by ring closure in the initial adduct **i99**. From the intermediates **i109** and **i113**, a carbon−carbon single bond cleavage in the CH_2CH fragment of the four-member ring in the former and an H migration from the non-terminal CH_2 group to the adjacent terminal CH_2 moiety in the latter access two conformers **i31** and **i15**, which are linked to one another *via* a moderate rotational barrier of 34 kJ mol^{-1}. The five-member **i9** and three-member **i101** cyclic intermediates are both connected to the three-member ring structure **i57**. The intermediate **i102** can isomerize to **i45**, which in turn easily rotates to its conformer **i8**. The latter can be also formed by hydrogen shifts from the CH_3 group to the opposite CH moiety in **i105** and from the CH group to the adjacent bare carbon atom in **i113**. The structures **i36** and **i116** are connected by an H migration from the CH_2 group to the adjacent bare carbon. The intermediates **i8**, **i30**, and **i102**, for their part, can produce **i14** *via* different hydrogen shifts.

$$\begin{aligned} &CH + CH_3CH_2CCH \rightarrow [\mathbf{i98} \rightarrow \mathbf{i9}] \\ &\quad /[\mathbf{i99} \rightarrow \mathbf{i103}/\mathbf{i104} \rightarrow \mathbf{i98}]/[\mathbf{i98}/\mathbf{i99} \rightarrow \mathbf{i103} \rightarrow \mathbf{i30} \\ &\quad \rightarrow \mathbf{i5}]/[\mathbf{i100} \rightarrow \mathbf{i30}/\mathbf{i113} \rightarrow \mathbf{i5}] \rightarrow \mathbf{i6} \rightarrow \mathbf{p1} + H \end{aligned} \tag{15}$$

Pathways Leading to Intermediates i38, i48, i50, i52, i65, and i81. As seen in Figure 5, a C−C single bond formation between the non-terminal CH group and the bare carbon in **i103** or between the CH_2 group and the bare C atom in **i99** forms a three-member ring isomer **i114** *via* barriers of 80 and 69 kJ mol^{-1}, respectively. Furthermore, **i114** can isomerize to the four-member cyclic intermediate **i109**, which can also be obtained directly from the initial adduct **i99**. **i109** can further rearrange to the rhombic **i110** structure, which in turn moves on to **i48**, a three-member ring isomer representing one of the initial adducts of the CH + 1,2-butadiene reaction. **i48** can also be formed from **i101**, whereas **i107** gives rise to another three-member ring isomer **i38**. Besides, **i114** can produce other two cyclic intermediates **i52** and **i81**. A C−C bond rupture in the *c*-$CCCH_2$ moiety of **i106** or the C_2H_5 group migration in **i102** results in an acyclic structure **i115**, which again undergoes a three-member ring closure to form **i50**, yet another initial adduct of CH + 1,2-butadiene.[25] **i50** can also form from the rhombic **i110** structure. Finally, the intermediate **i115** can transform to the three-member ring structure **i65** by 1,3-CH_3 migration accompanied by cyclization. Although we do not expect the reaction channels illustrated in Figure 5 to play a significant role in the CH + 1-butyne reaction, this part of the PES displays the connections between the areas of the C_5H_7 surface accessed by the CH reactions with 1-butyne and 1,2-butadiene, especially through the formation of a broad variety of three-member ring isomers.

Statistical Product Branching Ratios. Our current kinetic scheme involving the C_5H_7 PES incorporates all intermediates, transition states, and bimolecular products studied earlier for CH reactions with the other C_4H_6 isomers, with addition of those investigated here for the CH + 1-butyne reaction. This kinetic scheme was utilized to compute statistical yields of various products **p1**−**p51** using RRKM theory (Table 1) at the zero-pressure limit corresponding to the conditions of crossed molecular beam experiments and those in cold molecular clouds. The computed rate constants are presented in Table S2 of Supporting Information. We considered all possible CH + 1-butyne entrance channels including methylidyne insertions into various C−H bonds,

https://doi.org/10.1021/acs.jpca.1c07519
J. Phys. Chem. A 2021, 125, 9536−9547

although these pathways are expected to be much less likely than the CH radical addition to the triple C≡C bond.[38−41] According to the results, with **i98** and **i117** as the initial adducts obtained by CH insertion in a C−H bond in the methyl group of 1-butyne, ethylene (**p24**, 84.3%) is the most likely product along with the propargyl radical, while 4-penten-1-yne (**p4**, **p7**, and **p36**, 4.2% for each conformer) is a minor product. If the CH radical inserts into a C−H bond of the CH_2 group in the C_2H_5 moiety forming the **i99** initial adduct, the vinylacetylene + methyl radical products (**p23**, 55.2%) prevail, whereas the C_5H_6 products—all formed upon an H loss from C_5H_7 intermediates, 4-penten-1-yne (**p4**, 6.4%; **p7**, 4.8%; and **p36**, 6.3%), (*Z*)-3-penten-1-yne (**p9**, 6.1%), (*E*)-3-penten-1-yne (**p15**, 7.3%), and 2-methyl-1-buten-3-yne (**p30**, 10.6%)—contribute less. Insertion into the terminal acetylenic C−H bond in 1-butyne to produce **i102** is the least likely mechanism, but it was also considered here. In this case, 1,2,3-butatriene plus the methyl radical (**p35**, 84.0%) dominate the overall product yield, with 1,2,3-pentatriene + H (**p10**, 11.2%) as the main minor product. When it comes to addition to the terminal carbon in 1-butyne forming metastable **i100**, methylenecyclopropene + methyl radical (**p32**, 41.4%) and cyclopropenylidene + ethyl radical (**p47**, 20.6%) are the major products, whereas cyclopentadiene + H (**p1**, 8.5%), (*Z*)-3-penten-1-yne + H (**p9**, 4.8%), 3-ethylidenecyclopropene + H (**p16**, 5.8%), and 1,2,3-butatriene + methyl radical (**p35**, 9.2%) give small contributions. If the methylidyne radical adds to the triple C≡C bond of 1-butyne giving **i101** as the initial adduct, methylenecyclopropene + methyl radical (**p32**, 54.7%) and cyclopropenylidene + ethyl radical (**p47**, 27.2%) dominate the product yield, with minor contributions from 3-ethylidenecyclopropene + H (**p16**, 7.6%) and 1,2,3-butatriene + methyl radical (**p35**, 5.8%). Clearly, for all initial reaction scenarios, the C_5H_6 + H products give only minor contributions, whereas the decomposition of the C_5H_7 intermediates into heavy fragments, in particular, *via* propargyl, methyl, and ethyl radical losses are prevalent.

Identification of the Main Reaction Channels. With the computed statistical branching ratios in hand, we can now identify the most important channels of the CH + 1-butyne reaction (Figure 6). From **i98** and **i117**, the ethylene + propargyl radical (**p24**) is formed directly, *via* a C−C bond *β*-scission process overcoming a barrier of 101 kJ mol^{-1} (channel 8). The minor products, 4-penten-1-yne + H (in three different conformers **p4**, **p7**, and **p36**), are also produced directly *via* C−H bond *β*-scission *via* higher barriers of 153 kJ mol^{-1} for **p7** in channel 7 and 158 kJ mol^{-1} for **p4** and **p36** in channel 10. With **i99** as the initial adduct, the predominant products, vinylacetylene + CH_3 (**p23**), are also formed directly, by C−C bond *β*-scission *via* a 122 kJ mol^{-1} barrier (channel 5). Alternatively, a significant number of minor products can be produced as well: 4-penten-1-yne + H (**p4**/**p36**) and (*E*)-3-penten-1-yne + H (**p15**) indirectly *via* **i116**—channel 10, 4-penten-1-yne + H (**p7**) *via* **i103** and **i98**—channel 7, (*Z*)-3-penten-1-yne + H (**p9**) *via* **i30**, **i103**, and **i105**—channel 9, and 2-methyl-1-buten-3-yne + H (**p30**) *via* **i99**—channel 6. Considering **i100** as the initial complex of CH addition to the terminal acetylenic carbon, the main products methylenecyclopropene + CH_3 (**p32**) and cyclopropenylidene + ethyl (**p47**) and minor 3-ethylidene-cyclopropene + H (**p16**) are produced via channel 3, CH + CH_3CH_2CCH → **i100** → **i101** → **i107** → **p16** + H/**p32** + CH_3/**p47** + C_2H_5. The other significant minor products include cyclopentadiene + H (**p1**) *via* CH + CH_3CH_2CCH → **i100** → **i30**/**i113** → **i5** → **i6** → **p1** + H—channel 15, (*Z*)-3-penten-1-yne + H (**p9**) *via* CH + CH_3CH_2CCH → **i100** → [**i30**]/[**i101** → **i105**] → **p9** + H—channel 9, and 1,2,3-butatriene + CH_3 (**p35**) *via* CH + CH_3CH_2CCH → **i100** → **i101**→ **i106** → **i102** → **p35** + CH_3—channel 4. The prevailing channels are nearly the same when **i101** is the initial complex produced by methylidyne addition to the triple C≡C bond of 1-butyne because **i100** is metastable with respect to its ring closure to **i101**. The main exceptions are very low yields of **p1** and **p9** because the channels to these products involve isomerizations of **i100** to **i113** and **i105**, respectively, which are hindered by sizeable barriers. The reduced yields of **p1** and **p9** from **i101** as compared to those from **i100** are compensated by the higher yields of the two major products, **p32** and **p47**. Finally, if **i102** happens to be the initial adduct produced by CH insertion into the acetylenic C−H bond; the dominant 1,2,3-butatriene + CH_3 (**p35**) and minor 1,2,3-pentatriene + H (**p10**) products are formed directly *via* channel 4, CH + CH_3CH_2CCH → **i102** → **p10** + H/**p35** + CH_3, involving C−C and C−H bond *β*-scissions *via* barriers of 194 and 221 kJ mol^{-1}, respectively.

It is anticipated from the previous studies of CH reactions with unsaturated hydrocarbons that the most favorable entrance channel should be CH addition to the triple C≡C bond followed by CH insertion to a C−H bond of the terminal sp^3 carbon atom.[38−43] In this view, we expect that the prevailing reaction outcome should be the formation methylenecyclopropene + CH_3 (**p32**), cyclopropenylidene + ethyl (**p47**), and ethylene + propargyl (**p24**), with a rather minor expected yield of C_5H_6 + H. Therefore, crossed molecular beam experiments on CH + 1-butyne are anticipated to be difficult due to a low signal-to-noise ratio. Kinematically, it is easier in a crossed beam experiment to detect a heavy product of an H atom loss than to observe dissociation to two heavy fragments, which are often masked by the products of dissociative ionization of the initial reactants, here C_4H_6.

■ CONCLUSIONS

Ab initio calculations of the C_5H_7 PES combined with RRKM calculations of product branching ratios at the zero pressure limit allowed us to unravel the mechanism of the reaction of the methylidyne radical with the C_4H_6 isomer 1-butyne under conditions of crossed molecular beam experiments and in cold molecular clouds. The results indicate that in the entrance reaction channel, CH can either add to the triple C≡C bond or to the terminal acetylenic carbon atom, forming the initial adducts **i101** and **i100**, where the latter is unstable with respect to spontaneous three-member ring closure to **i101**. Alternatively, CH insertion into C−H bonds in CH_3, CH_2, or CH groups of 1-butyne can produce the initial adducts **i98**/**i117**, **i99**, or **i102**, respectively. Following the triple addition forming **i101**, the reaction most likely produces the methylenecyclopropene + methyl CH_3 (**p32**) and cyclopropenylidene + ethyl C_2H_5 (**p47**) roughly in a 2:1 ratio. Alternatively, CH insertion into a C−H bond in the methyl group of 1-butyne via **i98**/**i117** is predicted to preferentially form ethylene + propargyl (**p24**) by the C−C bond *β*-scission in the initial complex, whereas CH insertion into C−H of the CH_2 group *via* **i99** would predominantly produce vinylacetylene + CH_3 (**p23**) also by the C−C bond *β*-scission in the adduct. If a minor reaction flux proceeds by CH insertion into the acetylenic CH group in 1-butyne to **i102**, the prevalent product is predicted to be 1,2,3-butatriene + CH_3. In all cases, the formation of any

https://doi.org/10.1021/acs.jpca.1c07519
J. Phys. Chem. A 2021, 125, 9536−9547

C_5H_6 isomers *via* H loss from C_5H_7 intermediates is expected to represent only minor reaction pathways. Therefore, while the CH + 1-butyne reaction is expected to be facile in cold molecular clouds, it is not anticipated to result in the growth of the carbon skeleton. Instead, it is likely to lead to less saturated C_4 molecules like C_4H_4 isomers methylenecyclopropene, vinylacetylene, and 1,2,3-butatriene and even smaller C_2 and C_3 hydrocarbons including methyl, ethyl, and propargyl radicals, ethylene, and exotic cyclopropenylidene. The present study confirms a very strong dependence of the reaction products on the isomeric structure of the C_4H_6 molecule explained by the fact that the preferable reaction mechanism normally involves a rapid decomposition of the initial reaction collision complexes (adducts), whose structure is controlled by the isomeric form of the reactant.

■ ASSOCIATED CONTENT

Supporting Information

The Supporting Information is available free of charge at https://pubs.acs.org/doi/10.1021/acs.jpca.1c07519.

Optimized Cartesian coordinates and calculated vibrational frequencies for the reactants, products, intermediates, and transition states involved in the CH + 1-butyne reaction and RRKM-calculated rate constants for unimolecular reaction steps (PDF)

■ AUTHOR INFORMATION

Corresponding Author

Alexander M. Mebel − *Department of Chemistry and Biochemistry, Florida International University, Miami, Florida 33199, United States;* orcid.org/0000-0002-7233-3133; Email: mebela@fiu.edu

Authors

Anatoliy A. Nikolayev − *Lebedev Physical Institute, Samara 443011, Russian Federation; Samara National Research University, Samara 443086, Russian Federation*

Valeriy N. Azyazov − *Lebedev Physical Institute, Samara 443011, Russian Federation; Samara National Research University, Samara 443086, Russian Federation*

Ralf I. Kaiser − *Department of Chemistry, University of Hawai'i at Manoa, Honolulu, Hawaii 96822, United States;* orcid.org/0000-0002-7233-7206

Complete contact information is available at: https://pubs.acs.org/10.1021/acs.jpca.1c07519

Notes

The authors declare no competing financial interest.

■ ACKNOWLEDGMENTS

This work was supported by the U.S. Department of Energy, Basic Energy Sciences DE-FG02-04ER15570 and DE-FG02-03ER15411 to Florida International University and to the University of Hawaii, respectively. Ab initio calculations at the Lebedev Physics Institute were supported by the Ministry of Higher Education and Science of the Russian Federation under grant No. 075-15-2021-597.

■ REFERENCES

(1) Hansen, N.; Klippenstein, S. J.; Miller, J. A.; Wang, J.; Cool, T. A.; Law, M. E.; Westmoreland, P. R.; Kasper, T.; Kohse-Höinghaus, K. Identification of C_5H_x Isomers in Fuel-Rich Flames by Photoionization Mass Spectrometry and Electronic Structure Calculations. *J. Phys. Chem. A* **2006**, *110*, 4376−4388.

(2) Hansen, N.; Miller, J. A.; Taatjes, C. A.; Wang, J.; Cool, T. A.; Law, M. E.; Westmoreland, P. R. Photoionization Mass Spectrometric Studies and Modeling of Fuel-Rich Allene and Propyne Flames. *Proc. Combust. Inst.* **2007**, *31*, 1157−1164.

(3) Yang, B.; Huang, C.; Wei, L.; Wang, J.; Sheng, L.; Zhang, Y.; Qi, F.; Zheng, W.; Li, W.-K. Identification of Isomeric C_5H_3 and C_5H_5 Free Radicals in Flame with Tunable Synchrotron Photoionization. *Chem. Phys. Lett.* **2006**, *423*, 321−326.

(4) Cernicharo, J.; Kahane, C.; Gomez-Gonzalez, J.; Guélin, M. Detection of the $^2\Pi_{3/2}$ State of C_5H. *Astron. Astrophys.* **1986**, *167*, L5−L7.

(5) Cernicharo, J.; Kahane, C.; Gomez-Gonzalez, J.; Guélin, M. Tentative Detection of the C_5H Radical. *Astron. Astrophys.* **1986**, *164*, L1−L4.

(6) Cernicharo, J.; Guélin, M.; Walmsley, C. M. Detection of the Hyperfine Structure of the C_5H Radical. *Astron. Astrophys.* **1987**, *172*, L5−L6.

(7) Bernath, P. F.; Hinkle, K. H.; Keady, J. J. Detection of C_5 in the Circumstellar Shell of IRC+10216. *Science* **1989**, *244*, 562−564.

(8) Hahndorf, I.; Lee, H. Y.; Mebel, A. M.; Lin, S. H.; Lee, Y. T.; Kaiser, R. I. A Combined Crossed Beam and Ab Initio Investigation on the Reaction of Carbon Species with C_4H_6 Isomers. I. The 1,3-Butadiene Molecule, $H_2CCHCHCH_2(X^1A')$. *J. Chem. Phys.* **2000**, *113*, 9622−9636.

(9) Huang, L. C. L.; Lee, H. Y.; Mebel, A. M.; Lin, S. H.; Lee, Y. T.; Kaiser, R. I. A Combined Crossed Beam and Ab Initio Investigation on the Reaction of Carbon Species with C_4H_6 Isomers. II. The Dimethylacetylene Molecule, $H_3CCCCH_3(X^1A_{1g})$. *J. Chem. Phys.* **2000**, *113*, 9637−9648.

(10) Balucani, N.; Lee, H. Y.; Mebel, A. M.; Lee, Y. T.; Kaiser, R. I. A Combined Crossed Beam and Ab Initio Investigation on the Reaction of Carbon Species with C_4H_6 Isomers. III. 1,2-Butadiene, $H_2CCCH(CH_3)(X^1A')$—a non-Rice-Ramsperger-Kassel-Marcus System? *J. Chem. Phys.* **2001**, *115*, 5107−5116.

(11) Guo, Y.; Gu, X.; Balucani, N.; Kaiser, R. I. Formation of the 2,4-Pentadiynyl-1 Radical ($H_2CCCCCH$, X^2B_1) in the Crossed Beams Reaction of Dicarbon Molecules with Methylacetylene. *J. Phys. Chem. A* **2006**, *110*, 6245−6249.

(12) Guo, Y.; Gu, X.; Zhang, F.; Mebel, A. M.; Kaiser, R. I. Unimolecular Decomposition of Chemically Activated Pentatetraene ($H_2CCCCCH_2$) Intermediates: A Crossed Beams Study of Dicarbon Molecule Reactions with Allene. *J. Phys. Chem. A* **2006**, *110*, 10699−10707.

(13) Mebel, A. M.; Kislov, V. V.; Kaiser, R. I. Potential Energy Surface and Product Branching Ratios for the Reaction of Dicarbon, C_2 ($X^1\Sigma_g^+$), with Methylacetylene, CH_3CCH (X^1A_1): An Ab Initio/RRKM Study. *J. Phys. Chem. A* **2006**, *110*, 2421−2433.

(14) Gu, X.; Guo, Y.; Zhang, F.; Mebel, A. M.; Kaiser, R. I. Unimolecular Decomposition of Chemically Activated Singlet and Triplet D3-Methyldiacetylene Molecules. *Chem. Phys. Lett.* **2007**, *444*, 220−225.

(15) Parker, D. S. N.; Zhang, F.; Kim, Y. S.; Kaiser, R. I.; Mebel, A. M. On the Formation of Resonantly Stabilized C_5H_3 Radicals − A Crossed Beam and Ab Initio Study of the Reaction of Ground State Carbon Atoms with Vinylacetylene. *J. Phys. Chem. A* **2011**, *115*, 593−601.

(16) Dangi, B. B.; Maity, S.; Kaiser, R. I.; Mebel, A. M. A Combined Crossed Beam and Ab Initio Investigation of the Gas Phase Reaction of Dicarbon Molecules (C_2; $X^1\Sigma_g^+/a^3\Pi_u$) with Propene (C_3H_6; X^1A'): Identification of the Resonantly Stabilized Free Radicals 1- and 3-Vinylpropargyl. *J. Phys. Chem. A* **2013**, *117*, 11783−11793.

(17) Gong, C.-M.; Ning, H.-B.; Li, Z.-R.; Li, X.-Y. Theoretical and Kinetic Study of Reaction $C_2H + C_3H_6$ on the C_5H_7 Potential Energy Surface. *Theor. Chem. Acc.* **2015**, *134*, 1599.

(18) da Silva, G. Mystery of 1-Vinylpropargyl Formation from Acetylene Addition to the Propargyl Radical: an Open-and-Shut Case. *J. Phys. Chem. A* **2017**, *121*, 2086−2095.

(19) Thomas, A. M.; Lucas, M.; Zhao, L.; Liddiard, J.; Kaiser, R. I.; Mebel, A. M. A Combined Crossed Molecular Beams and Computational Study on the Formation of Distinct Resonantly Stabilized C_5H_3 Radicals via Chemically Activated C_5H_4 and C_6H_6 Intermediates. *Phys. Chem. Chem. Phys.* **2018**, *20*, 10906−10925.
(20) Thomas, A. M.; Zhao, L.; He, C.; Mebel, A. M.; Kaiser, R. I. A Combined Experimental and Computational Study on the Reaction Dynamics of the 1-Propynyl (CH_3CC)—Acetylene (HCCH) System and the Formation of Methyldiacetylene (CH_3CCCCH). *J. Phys. Chem. A* **2018**, *122*, 6663−6672.
(21) He, C.; Zhao, L.; Thomas, A. M.; Galimova, G. R.; Mebel, A. M.; Kaiser, R. I. A Combined Experimental and Computational Study on the Reaction Dynamics of the 1-Propynyl Radical (CH_3CC; X^2A_1) with Ethylene (H_2CCH_2; X^1A_{1g}) and the Formation of 1-penten-3-yne ($CH_2CHCCCH_3$; X^1A'). *Phys. Chem. Chem. Phys.* **2019**, *21*, 22308−22319.
(22) Kaiser, R. I.; Hansen, N. An Aromatic Universe—A Physical Chemistry Perspective. *J. Phys. Chem. A* **2021**, *125*, 3826−3840.
(23) Zhang, F.; Kim, Y. S.; Zhou, L.; Chang, A. H. H.; Kaiser, R. I. A Crossed Molecular Beam Study on the Synthesis of the Interstellar 2,4-Pentadiynylidyne Radical (HCCCCC). *J. Chem. Phys.* **2008**, *129*, 134313.
(24) He, C.; Zhao, L.; Doddipatla, S.; Thomas, A. M.; Nikolayev, A. A.; Galimova, G. R.; Azyazov, V. N.; Mebel, A. M.; Kaiser, R. I. Gas-Phase Synthesis of 3-Vinylcyclopropene via the Crossed Beam Reaction of the Methylidyne Radical (CH; $X^2\Pi$) with 1,3-Butadiene ($CH_2CHCHCH_2$; X^1A_g). *ChemPhysChem* **2020**, *21*, 1295−1309.
(25) He, C.; Nikolayev, A. A.; Zhao, L.; Thomas, A. M.; Doddipatla, S.; Galimova, G. R.; Azyazov, V. N.; Mebel, A. M.; Kaiser, R. I. Gas-Phase Formation of C_5H_6 Isomers via the Crossed Molecular Beam Reaction of the Methylidyne Radical (CH; $X^2\Pi$) with 1,2-Butadiene (CH_3CHCCH_2; X^1A'). *J. Phys. Chem. A* **2021**, *125*, 126−138.
(26) Chai, J.-D.; Head-Gordon, M. Long-Range Corrected Hybrid Density Functionals with Damped Atom-Atom Dispersion Corrections. *Phys. Chem. Chem. Phys.* **2008**, *10*, 6615−6620.
(27) Adler, T. B.; Knizia, G.; Werner, H.-J. A Simple and Efficient CCSD(T)-F12 approximation. *J. Chem. Phys.* **2007**, *127*, 221106.
(28) Knizia, G.; Adler, T. B.; Werner, H.-J. Simplified CCSD(T)-F12 Methods: Theory and Benchmarks. *J. Chem. Phys.* **2009**, *130*, 054104.
(29) Dunning, T. H., Jr. Gaussian Basis Sets for Use in Correlated Molecular Calculations. I. The Atoms Boron through Neon and Hydrogen. *J. Chem. Phys.* **1989**, *90*, 1007−1023.
(30) Zhang, J.; Valeev, E. F. Prediction of Reaction Barriers and Thermochemical Properties with Explicitly Correlated Coupled-Cluster Methods: A Basis Set Assessment. *J. Chem. Theory Comput.* **2012**, *8*, 3175−3186.
(31) Frisch, M. J.; Trucks, G. W.; Schlegel, H. B.; Scuseria, G. E.; Robb, M. A.; Cheeseman, J. R.; Scalmani, G.; Barone, V.; Mennucci, B.; Petersson, G. A.; et al. *Gaussian 09*; Revision A.1; Gaussian, Inc.: Wallingford CT, 2009.
(32) Werner, H.-J.; Knowles, P. J.; Lindh, R.; Manby, F. R.; Schütz, M.; Celani, P.; Korona, T.; Rauhut, G.; Amos, R. D.; Bernhardsson, A. *MOLPRO, A Package of Ab Initio Programs*; version 2010.1; University of Cardiff: Cardiff: U.K.., 2010.
(33) Steinfeld, J. I.; Francisco, J. S.; Hase, W. L.. *Chemical Kinetics and Dynamics*; Prentice Hall: Englewood Cliffs, NJ, 1982; Vol. 3.
(34) Hofacker, G. L. Henry Eyring, S. H. Lin, S. M. Lin: Basic Chemical Kinetics. John Wiley & Sons, New York, Chichester, Brisbane, Toronto 1980. 493 Seiten, Preis: £ 20. *Phys Chem Chem Phys* **1981**, *85*, 618−619 John Wiley and Sons, Inc.: New York, 1980.
(35) Robinson, P. J.; Holbrook, K. A. *Unimolecular Reactions*; Wiley: New York, 1972.
(36) He, C.; Zhao, L.; Thomas, A. M.; Morozov, A. N.; Mebel, A. M.; Kaiser, R. I. Elucidating the Chemical Dynamics of the Elementary Reactions of the 1-Propynyl Radical (CH_3CC; X^2A_1) with Methylacetylene (H_3CCCH; X^1A_1) and allene (H_2CCCH_2; X^1A_1). *J. Phys. Chem. A* **2019**, *123*, 5446−5462.
(37) Kislov, V. V.; Nguyen, T. L.; Mebel, A. M.; Lin, S. H.; Smith, S. C. Photodissociation of Benzene under Collision-Free Conditions: An Ab Initio/Rice-Ramsperger-Kassel-Marcus Study. *J. Chem. Phys.* **2004**, *120*, 7008−7017.
(38) Maksyutenko, P.; Zhang, F.; Gu, X.; Kaiser, R. I. A Crossed Molecular Beam Study on the Reaction of Methylidyne Radicals [$CH(X^2\Pi)$] with Acetylene [$C_2H_2(X^1\Sigma_g^+)$]—competing C_3H_2+H and C_3H+H_2 channels. *Phys. Chem. Chem. Phys.* **2011**, *13*, 240−252.
(39) Kaiser, R. I.; Gu, X.; Zhang, F.; Maksyutenko, P. Crossed Beam Reactions of Methylidyne [$CH(X^2\Pi)$] with D2-Acetylene [$C_2D_2(X1\Sigma_g^+)$] and of D1-Methylidyne [$CD(X^2\Pi)$] with Acetylene [$C_2H_2(X^1\Sigma_g^+)$]. *Phys. Chem. Chem. Phys.* **2012**, *14*, 575−588.
(40) Ribeiro, J. M.; Mebel, A. M. Reaction Mechanism and Product Branching Ratios of the CH+C_3H_4 Reactions: A Theoretical Study. *Phys. Chem. Chem. Phys.* **2017**, *19*, 14543−14554.
(41) Ribeiro, J. M. Kinetics and Reaction Mechanisms for Methylidyne Radical Reactions with Small Hydrocarbons. Doctoral Dissertation, Florida International University: Miami, 2016. https://digitalcommons.fiu.edu/etd/3023.
(42) Ribeiro, J. M.; Mebel, A. M. Reaction Mechanism and Product Branching Ratios of the CH+C_3H_8 Reaction: A Theoretical Study. *J. Phys. Chem. A* **2014**, *118*, 9080−9086.
(43) Ribeiro, J. M.; Mebel, A. M. Reaction Mechanism and Product Branching Ratios of the CH+C_3H_6 Reaction: A Theoretical Study. *J. Phys. Chem. A* **2016**, *120*, 1800−1812.

https://doi.org/10.1021/acs.jpca.1c07519
J. Phys. Chem. A 2021, 125, 9536−9547